Journal of Alloys and Compounds 550 (2013) 358–364

Contents lists available at SciVerse ScienceDirect

Journal of Alloys and Compounds

journal homepage: www.elsevier.com/locate/jalcom

Structural, magnetic and magnetocaloric properties of $La_{0.8}Ba_{0.2}Mn_{1-x}Fe_xO_3$ compounds with $0 \leqslant x \leqslant 0.1$

S. Ghodhbane [a,*], A. Dhahri [a], N. Dhahri [a], E.K. Hlil [b], J. Dhahri [a]

[a] Laboratoire de la matière condensée et des nanosciences, Département de Physique, Faculté des Sciences, Université de Monastir, Monastir 5019, Tunisia
[b] Institut Néel, CNRS-Université J. Fourier, BP 166, 38042 Gronoble, France

ARTICLE INFO

Article history:
Received 31 August 2012
Received in revised form 15 October 2012
Accepted 18 October 2012
Available online 2 November 2012

Keywords:
Perovskites
Magnetic entropy
Magnetocaloric effect
Critical phenomena

ABSTRACT

The present study reports the effect of Fe doping on the structural, magnetic and magnetocaloric proprieties in the $La_{0.8}Ba_{0.2}Mn_{1-x}Fe_xO_3$ ($0 \leqslant x \leqslant 0.1$) perovskites. The studied samples were synthesized as powder samples by solid state reaction at high temperature. Their analysis by powder X-ray diffraction using Rietveld refinement showed that they crystallize in the rhombohedral system with the R3C space group. They display a paramagnetic (PM)-ferromagnetic (FM) phase transition with decreasing temperature. All of them exhibit a maximum and large magnetocaloric effect near the Curie temperature (T_C). The magnitude of the isothermal magnetic entropy $|\Delta S_M^{max}|$ at the FM Curie temperature decreases from 4.15 J kg^{-1} K^{-1} for the $x = 0$ composition to 2.62 J kg^{-1} K^{-1} for $x = 0.1$, for a magnetic field change of 5T. For an applied magnetic field of 5T, the relative cooling power (RCP) values are found to vary between 211 and 238 J kg^{-1}. The phenomenon of large entropy change and the convenient adjustment of the Curie temperature make these peroskite-type manganese oxides useful for magnetic refrigeration in an extended high temperature range even at room temperature.

1. Introduction

Magnetic refrigeration is a kind of cooling technology that uses a magnetic material as the working substance. It makes use of the magnetocaloric (MC) effect of the magnetic refrigerant material to obtain low temperatures. The MC effect has been applied widely for magnetic refrigeration technology with the aim of suppressing the emission of pollution components which appear in conventional refrigeration systems. Compared with the conventional gas refrigeration, the magnetic refrigeration has considerable advantages such as high efficiency, small volume, non pollution, etc. For a long time, gadolinium (Gd) with large magnetocaloric effect (MCE) has been considered as the most active magnetic refrigerant in room-temperature magnetic refrigerators [1–3] but its usage is somewhat commercially limited because the cost of Gd is quite expensive (~$4000/kg). Besides Gd, much effort in the search of new magnetic refrigerators has extended the possible candidates to a broad series of compounds such as $Gd_5(Si_xGe_{1-x})_4$ [4], Gd_2PdSi_3 [5], and $ErCo_2$ [6].

Recently, an intensive interest in perovskite-type manganese oxides (the so called manganite) $Re_{1-x}A_xMnO_3$ (Re is a rare earth ion and A is an alkaline earth) is prompted by the observation of colossal magnetoresistance (CMR) [7]. Because of some advantages compared to Gd and intermetallic alloys, such as low production cost, chemical stability, high resistivity (minimum Eddy current loss) [8] and no corrosion effect, manganites have attracted more attention as alternative candidates for magnetic refrigeration in the vicinity of room temperature. Among these, perovskite manganites with the general formula $Re_{1-x}A_xMnO_3$ (Re = trivalent rare earth, A = divalent ion) [9–12] are of special interest as they are known to possess interesting fundamental properties with potential device applicability. When the Re element is doped by various elements, a proportionate amount of Mn^{3+} with the electronic configuration ($3d^4, t_{2g}^3 \uparrow t_g^1 \uparrow, S = 2$) is replaced by Mn^{4+} witch the electronic configuration ($3d^3, t_{2g}^3 \uparrow t_g^0 \uparrow, S = 3/2$) creating holes in the e_g band [13]. Magnetic properties of the $Re_{1-x}A_xMnO_3$ phases are strongly affected by the Mn–O bond length and Mn–O–Mn bond angle controlled by the ionic radii of A and B site ions) and Mn^{3+}/Mn^{4+} ratio which modifies the double exchange (DE) and superexchange (SE) interactions [14,15]. The magnetic and transport properties of the system are then determined by the competition between (DE) and (SE). In manganites, it is possible to dope at both A and B sites. A-site doping is known to control the Mn^{3+}/Mn^{4+} ratio in the material. Compared with A-site doping, Mn-site doping is more important because it not only modifies the Mn^{3+}–O^{2-}–Mn^{4+} network but also brings the doped transition metal ions.

As a contribution to the investigation of manganite materials, we report here the study of the effect, on the structural, magnetic and magnetocaloric properties, of Fe-doping in the $La_{0.8}Ba_{0.2}Mn_{1-x}Fe_xO_3$ ($0 \leqslant x \leqslant 0.1$) polycrystalline samples.

* Corresponding author.
E-mail address: godhbane.sana@gmail.com (S. Ghodhbane).

0925-8388/$ - see front matter © 2012 Elsevier B.V. All rights reserved.
http://dx.doi.org/10.1016/j.jallcom.2012.10.087

2. Experimental

Polycrystalline samples with the general formula $La_{0.8}Ba_{0.2}Mn_{1-x}Fe_xO_3$ ($x = 0, 0.05, 0.1$) were prepared by the conventional solid-state reaction. For each sample, stoichiometric quantities of high-purity oxides La_2O_3, Fe_2O_3 and MnO_2 and barium carbonate $BaCO_3$ where weighed, thoroughly mixed and ground in an agate mortar, then preheated at 1173 K. After being reground to ensure its best homogeneity, the mixture was pressed in pellets then subjected to a final heating for 24 h at 1623 K with intervening grinding.

The surface morphology and elemental analysis of the samples were carried out by scanning electron microscopy (SEM) and energy dispersive X-ray technique (EDX), respectively. The structure and phase purity of the as-prepared samples were checked by powder X-ray diffraction (XRD) using CuK_α radiation ($\lambda = 1.5406$ Å) at room temperature. The patterns were recorded in the $10° \leqslant 2\theta \leqslant 120°$ angular range with a step of 0.0167° and counting time of 18 s per step. Structural analysis was carried out using the Rietveld structural refinement program FULLPROF software (Version 1.9c-May 2001-LLB-JRC) [16].

Magnetization (M) vs. temperature (T) and magnetisation vs. magnetic field (H) were measured using BS2 magnetometer developed in Louis Neel Laboratory of Grenoble.

3. Results and discussion

3.1. Scanning electron microscopy

EDX spectrum at room temperature of the $La_{0.8}Ba_{0.2}Mn_{0.9}Fe_{0.1}O_3$ ($x = 0.1$) sample is shown in Fig. 1. This spectrum reveals the presence of La, Ba, Fe, Mn and O elements, which confirms that there is no loss of any integrated element during sintering within experimental errors.

SEM micrograph of the sample is shown in the inset of Fig. 1. Morphology analysis of the micrograph revealed that the particles of the sample show some tendency towards agglomeration and the grain size is estimated to be mostly within (294–243 nm). The average grain size (G_S) can also be calculated from the XRD peaks using the Scherer formula:

$$G_S = \frac{0.9\lambda}{\beta \cos\theta} \quad (1)$$

where λ is the employed X-ray wavelength, θ is the most intense peak (104), and β is defined as $\beta^2 = \beta_m^2 - \beta_S^2$. Here, β_m is the experimental full width at half maximum (FWHM) and β_s is the FWHM of a standard silicon [17]. The as obtained (G_S) are estimated to be mostly of 98, 81 and 70 nm for the $x = 0$, $x = 0.05$ and $x = 0.1$ samples, respectively. Obviously, the particle sizes observed by SEM are several times larger than those calculated by XRD, which indicates that each particle observed by SEM consists of several crystallized grains.

3.2. X-ray diffraction

The diffraction patterns clearly show the synthesized compounds to form a single phase. The absence of other peaks demonstrates the solubility of Fe in the perovskite structure.

The structure refinement of $La_{0.8}Ba_{0.2}Mn_{1-x}Fe_xO_3$ ($x = 0$, 0.05 and 0.1) samples was performed in the hexagonal setting of the $R\bar{3}C$ space group. The results of refinement are listed in Table 1. In this table, are also reported the residuals for the weighted pattern R_{WP} the pattern R_P the structure factor R_F and the goodness of fit χ^2. Fig. 2 illustrates the observed, calculated and difference profiles for the $x = 0.1$ composition.

The cell volume is slightly increased from 359.72(2) Å^3 to 360.16(3) Å^3 then to 360.20(4) Å^3 as the x composition range increases from 0 to 0.05 than to 0.1. According to Jonker [18] and Ahn et al. [19], iron enters into samples as Fe^{3+}. As Mn^{3+} and Fe^{3+} have almost the same ionic radius of 0.645 Å [20], no noticeable structural change by Fe doping can be identified. Consequently, lattice effects on magnetic and magnetocaloric properties may be ignored in these materials.

The relationship between $\langle r_B \rangle$ and the Mn–O–Mn bond angle is confirmed by structural analysis (Table 2). The rhombohedral structure distortion, indicated by the increase of Godscrhmit tolerance factor (t_{factor}) with increasing Fe doping was found (as shown in Table 2). The tolerance factor is defined as $t_{factor} = (r_A + r_O)/\sqrt{2}(r_B + r_O)$ (r_A is the average ionic radius of La^{3+} and Ba^{2+}, r_o the ionic radius of O^{2-} and r_B is the average ionic radius of Mn^{3+} and Mn^{4+}), respectively, in the perovskite ABO_3 structure. t_{factor} is equal to 1 for a compound with an ideal perovskite structure. If $t_{factor} < 1$, the strain within the compound is increased. Therefore, the t_{factor} increases with the addition of Fe giving rise to a release of the strain for $La_{0.8}Ba_{0.2}Mn_{1-x}Fe_xO_3$ and a decrease of the mean steric distortion D with increasing $\langle r_B \rangle$ (see Table 2). The steric distortion D is given by:

$$D = \frac{1}{3}\sum_i \left|\frac{a_i - \overline{a}}{a_i}\right| \times 100 \quad (2)$$

where $\overline{a} = (a_1 a_2 a_3)^{1/3}$, $a_1 = a_2 = a$, $a_3 = c/\sqrt{6}$ [21]

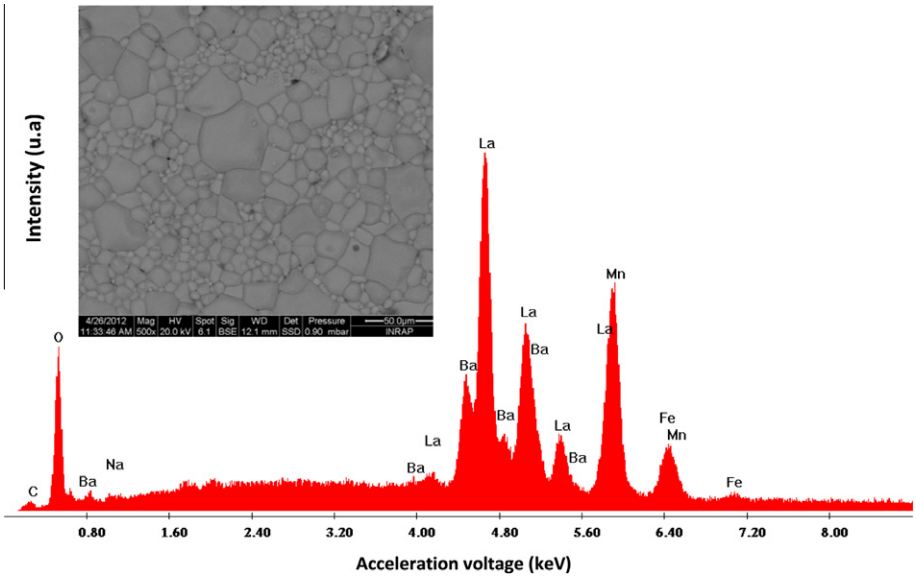

Fig. 1. Plot of EDX analysis of chemical species of $La_{0.8}Ba_{0.2}Mn_{1-x}Fe_xO_3$ with $x = 0.1$. The inset represents the scanning electron micrographs showing the transect surface morphology of pellets prepared in the same condition.